European Commission

JRC TECHNICAL REPORTS

Assessing the effects of extreme nutrients scenarios in European rivers for the ecosystem status of the Mediterranean Sea

Putting the Marine Modelling Framework to work

Macias, D., Stips, A., Garcia-Gorriz, E.

2018

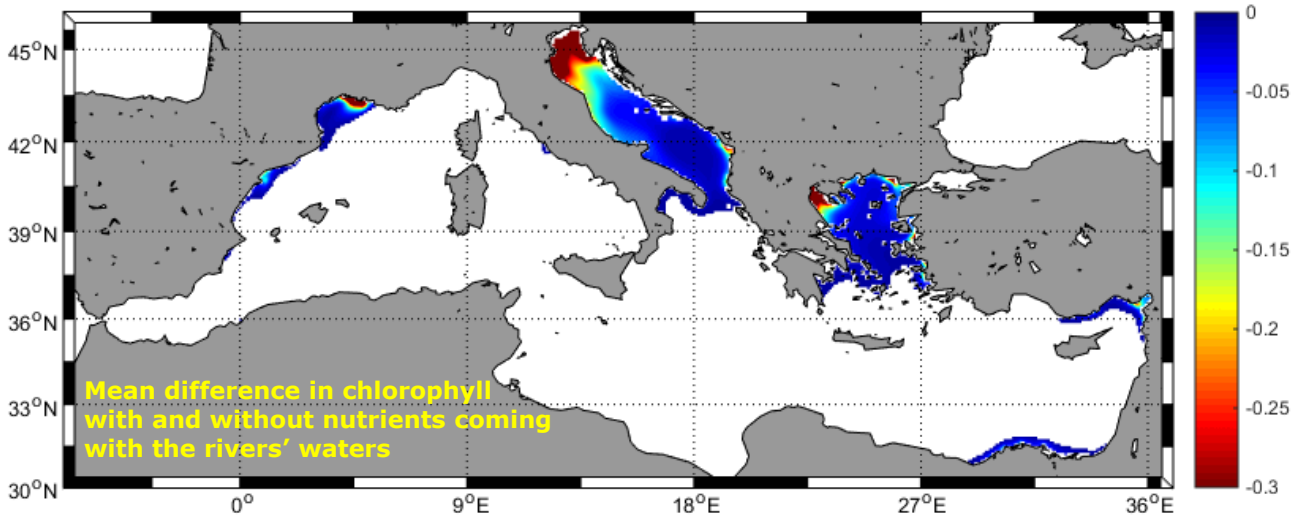

Joint Research Centre

EUR 29493 EN

Contact information
Name: Diego Macias
Address: Via E. Fermi, TP 270, 21020 Ispra, Italy
Email: diego.macias-moy@ec.europa.eu
Tel.: 0039 0332 78 9636

EU Science Hub
https://ec.europa.eu/jrc

JRC114157

EUR 29493 EN

PDF ISBN 978-92-79-98179-1 ISSN 1831-9424 doi:10.2760/045673

Luxembourg: Publications Office of the European Union, 2018

How to cite this report: Macias, D., Stips, A., Garcia-Gorriz, E., *Assessing the effects of extreme nutrients scenarios in European rivers for the ecosystem status of the Mediterranean Sea*, EUR 29493 EN, Publications Office of the European Union, Luxembourg, 2018, ISBN 978-92-79-98179-1, doi:10.2760/045673, JRC114157

Contents

Abstract

The main objective for the development of the Marine Modelling Framework (MMF) at the Joint Research Centre of the European Commission is the creation of a tool that allows evaluation of the impacts of policy options on the environmental status of EU regional seas. Within the remit of the MSFD AA (N° 11 06 61/ENV.C.2/2016/733192 & JRC No. 34131-2016 NFP) with DG Environment, one deliverable (#3.5) referred to '*A specific technical report will be produced summarizing the potential impacts of MS programs of measures on key environmental parameters including a gap analysis in relation to the targets set by each MS'*. As the program of measures from MS are still not available, the JRC marine modelling team designed a set of simulations to test the potentialities of the MMF to simulate the effects of different eutrophication scenarios in EU rivers. Here, an extreme scenario concerning the chemical quality of EU rivers is evaluated for the period 1960 – 2013 and compared with the results of the 'standard' hindcast model run. The river scenario consists in a total clean-up of inorganic nutrients from the freshwater and constitutes an unrealistic lower boundary for any management strategy that could be implemented regarding freshwater quality in Europe. By comparing MMF simulations with the full nutrient loads in the rivers with this alternative scenario, the impact of allochthonous river-borne fertilization on Mediterranean ecosystems could be analyzed and quantified. Moreover, this comparison provides an envelope of the range of expected consequences any freshwater management plans could have on the ecosystems' status of marine waters downstream.

1 Introduction

The Mediterranean Sea is a semi-enclosed basin subjected to multiple stressors coming from its climate condition (being an evaporative, concentration basin), its average water circulation (which prevents large renovation of water) and the diverse and highly populated countries on its shores (with the developed European countries in the north and the developing North-African ones at the south). All these elements combine with the expected consequences of climate change making the Mediterranean basin a 'hotspot' especially sensible (Giorgi et al., 2006) and, hence, a very appropriate place to use as case study.

These are some of the main reasons why the Joint Research Centre (JRC) of the European Commission decided to start the implementation of a Regional Earth System Model (RESM) specifically designed to assess marine ecosystems' status in this particular basin. The Marine Modelling Framework (MMF) developed incorporates all the different elements that influence the regional climate such as the atmosphere, the rivers and the ocean as shown in Fig. 1.

Figure 1. Simplified diagram of Marine Modelling Framework

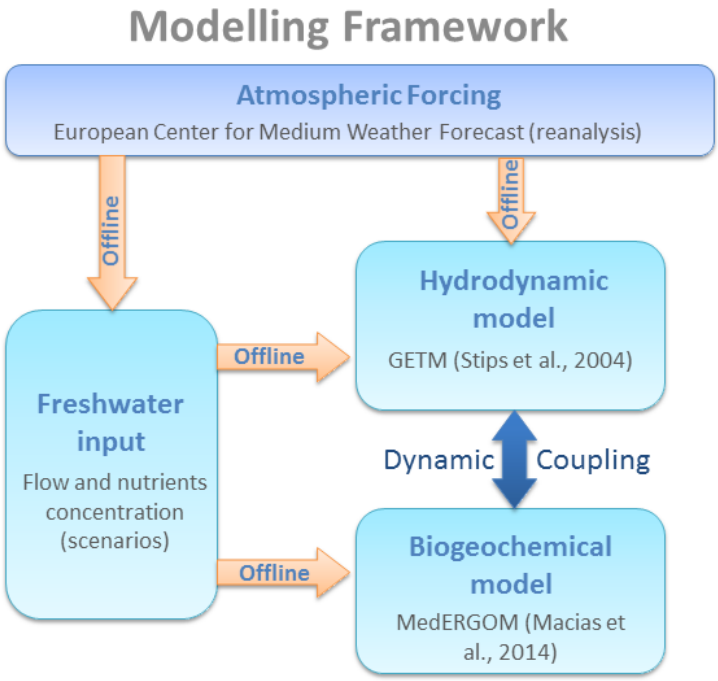

This MMF has been calibrated to properly represent current hydrodynamic and biogeochemical conditions in the Mediterranean basin and has been validated against all available information in previous applications (Macias et al., 2013; 2014a; 2014b; 2016a; 2018a). It has also been used to create some potential future scenarios for the ecosystems' status in the basin (Macias et al., 2015, 2016b, 2018b and 2018c) and so, it has become a valuable tool able to provide information about present, past and potential future state of the Mediterranean Sea ecosystems.

After all previous calibration and validation of the tools, they are on a mature state to simulate the impacts of measures on the ecosystems status of the Mediterranean Sea. Henceforth, and as stated in the memorandum of MSFD AA (N° 11 06 61/ENV.C.2/2016/733192 & JRC No. 34131-2016 NFP) the MMF should be used this year to create a technical report '*summarising the potential impacts of MS programs of measures on key environmental parameters including a gap analysis in relation to the*

targets set by each MS'. Unfortunately, the programs of measures for many MS are still lacking at the present time, so there is not enough quantitative information available to drive such simulations of the MMF. In this situation, the marine modelling team of JRC decided to design a hypothetical scenario to test the simulation capabilities of the MMF.

One main conclusion of previous works with the MMF was that riverine waters and, in particular, their chemical composition are fundamental drivers of the interannual variability of marine productivity in the Mediterranean Sea basin (see Macias et al., 2014b). Henceforth, and as the main aim at developing the MMF was to create a tool able to inform policy makers and stakeholders about potential impacts of management options on marine systems (see Stips et al., 2015) an extreme, low boundary scenario for nutrients fertilization by freshwater discharges has been created and tested in the present report. This scenario consists, basically, in removing all inorganic nutrients (nitrates and phosphates) from the rivers' waters and running the MMF for the whole hindcast period (1960 – 2013). By comparing the simulation in this model run with the 'standard' hindcast simulation (i.e., with inorganic nutrients in the rivers) the effects of allochthonous fertilization on marine ecosystems could be assessed on a quantitative way.

Henceforth, the comparison presented below, provides a lower boundary for any management option regarding freshwater inorganic nutrients loads, as a total removal of inorganic nutrients in rivers is not practicably achievable. Mean integrated changes in marine productivity and phytoplankton biomass as well as interannual and seasonal alterations are compared in the two evaluated runs. Hotspots of changes and most affected seasons are identified by applying statistical techniques, providing a maximum envelop to evaluate and interpret further scenarios for riverine waters quality to be tested in the near future.

2 Material and methods

2.1 Marine modelling framework

Here we use an integrated modelling framework developed at the JRC - Ispra of the EU Commission to specifically assess the consequences of different scenarios on the ecosystem status of regional European Seas (Stips et al. 2015). This MMF includes the main elements of a RESM, i.e., the atmosphere, the hydrological basin and the oceans (Fig. 1). By considering potential scenarios, the MMF allows to evaluate how political decisions and program of measures (for example regarding freshwater management) could affect the Good Environmental Status (GES) of the marine ecosystems downstream (e.g., Garcia-Gorriz et al. 2016).

2.1.1 Ocean

The oceanic component of the MMF is composed by two coupled models, a hydrodynamic model based on GETM (Burchard & Bolding, 2002) and a biogeochemical model based on ERGOM (Neumann, 2000). A detailed description of the GETM equations could be found in Stips et al. (2004) and at http://www.getm.eu. Our implementation for the Mediterranean Sea (Fig. 2) has a horizontal resolution of 5′ x 5′ (~9x9km) and includes 25 vertical sigma-layers. Model bathymetry was built using ETOPO1 (http://www.ngdc.noaa.gov/mgg/global/) database, while initial thermohaline conditions were created by using the Mediterranean Data Archeology and Rescue-MEDAR/MEDATLAS database (http://www.ifremer.fr/medar/). The same MEDAR/MEDATLAS data was used to create the boundary conditions for the model at the Strait of Gibraltar where monthly climatological vertically-explicit values of salinity and temperature are imposed. No horizontal currents are explicitly prescribed at the open boundary.

Figure 2. Model domain with bathymetric lines (background colour) and the position of the 53 rivers along the coast (red stars)

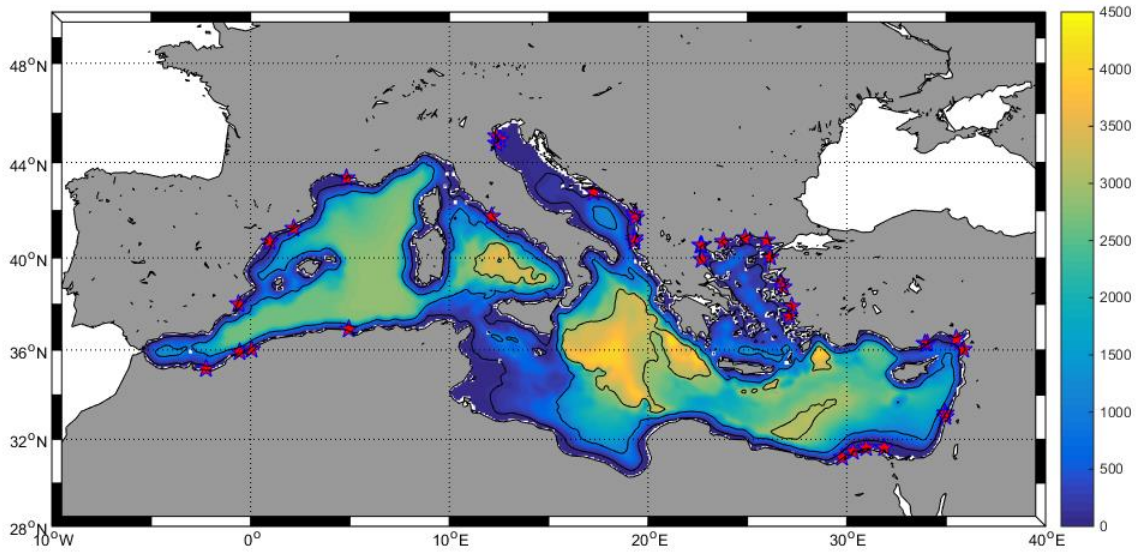

GETM is forced at the surface every 6 hours by the following atmospheric variables: wind velocity at 10 meters, air temperature at 2 m, dewpoint temperature at 2 m, cloud cover, atmospheric pressure at sea level and precipitation. Atmospheric data could come from reanalysis or from atmospheric models (see details below). In both cases, bulk formulae are used to calculate the corresponding relevant heat, mass and momentum fluxes between atmosphere and ocean (Macias et al., 2013).

GETM is coupled online to the MedERGOM biogeochemical model (Macias et al., 2014a and 2014b) by using the Framework for Aquatic Biogeochemical Models (FABM, https://sourceforge.net/projects/fabm/, Brueggeman & Bolding 2014). MedERGOM is a modified version of the ERGOM model (Neumann, 2000) specifically adapted to represent the conditions of the pelagic ecosystem of the Mediterranean Sea. Briefly, MedERGOM incorporates three phytoplankton functional types ('diatom-like', 'flagellates-like' and 'cyanobacteria-like'), two major nutrients (nitrate and phosphate), one zooplankton compartment and detritus. To get a more comprehensive description of this model the reader is referred to Macias et al. (2014a) and Macias et al. (2017). Biogeochemical initial and boundary conditions are computed from the World Ocean Atlas database (www.nodc.noaa.gov/OC5/indprod.html).

2.1.3 Atmosphere

The MMF described above incorporates the atmospheric component as an integral part of the RESM. As commented, this atmospheric compartment could be either a database (i.e., a reanalysis) or inputs from atmospheric models. For the present contribution we perform hindcast simulations covering the period 1960 – 2013 using the European Centre for Medium-Range Weather Forecasts (ECMWF) ERA-40 and ERAin databases. ERA-40 spans the period 1959 – 1979 while from 1979 onwards, ERAin is used. ECMWF databases provide relevant information on atmospheric conditions at an adequate horizontal resolution and have been shown to create reasonable ocean surface conditions in the Mediterranean Sea when used in combination with GETM (e.g., Macias et al., 2013).

2.1.3 Freshwater

The present configuration of the ocean model includes 53 rivers discharging along the Mediterranean coast (red stars in Fig 2). River inflow is treated as a boundary condition regarding water flow, temperature, salinity and nutrients (computed from the databases mentioned below) with respect to the grid cells where the river is entering. Once in the oceanic domain, the freshwater plume is subjected to the general hydrodynamic processes governing the water movements.

Values for river discharges were derived from the Global River Data Center (GRDC, Germany) database. Reducing the numbers of rivers to just 53 underestimates the total freshwater flow into the Mediterranean. These rivers provide a mean annual freshwater flow of ~309 km3/y which is lower than the total flow (including all rivers and creeks) computed by a state-of-the-art hydrological model (LISFLOOD, Burek et al., 2013) with a mean value of ~ 400 km3/y. However, we need to work with the reduced number of rivers in order to make the modelling system less costly to run in terms of computation time.

2.2 Rivers' scenarios

Two runs are performed for the period 1960 – 2013, which is the time-span covered by the ECMWF reanalysis data. The unique difference between the reference (or realistic) run (RR) and the 'no nutrients' run (RN) is on the nutrients (nitrate and phosphate) concentrations in riverine waters (see below). In both model runs, a continuous small atmospheric input of nitrate, phosphate and ammonium (equivalent to their climatological mean) is imposed in the entire model domain: nitrate ~ $8.0e^{-2}$ mmol/m^2d and ammonium ~ $4.0e^{-2}$ mmol/m^2d from EMEP (2015); phosphate ~$1.2e^{-3}$ mmol/m^2d assuming a N:P in the atmospheric deposition ~100 (Markaki et al., 2003).

For the RR, inorganic nutrient loads (nitrate and phosphate) of freshwater runoff were obtained from Ludwig et al. (2009) who combined literature reports with the Waterbase database at the European Environmental Agency (EAA) to get the most comprehensive, monthly-varying dataset on freshwater quality throughout Europe. However, this dataset is far from being complete, so we filled the existing gaps in the series by imposing the climatological concentration for the specific river and the concrete month computed from all available data.

Contrary, in the RN run a zero nutrient concentration in the freshwater was imposed for all rivers discharging in the Mediterranean basin. As the rest of conditions (boundaries, atmospheric forcing, etc..) remain unchanged, differences between RR and RN are only and exclusively due to the different nutrient loads in the freshwater flow. In both simulations, inorganic nutrients entering the Mediterranean Sea through Gibraltar and Bosphorous Straits are the same and based on best available data.

No other inputs of freshwater (and nutrients) such as point sources from large coastal cities are included in our model due to the lack of proper long-term datasets for such inputs. Ignoring these point sources in our simulations could make us underestimate the differences between the RR and RN runs.

2.3 Singular spectrum analysis

Some of the time-series of geophysical variables shown below have been analysed by a statistical methodology in order to extract the 'pure', independent signals hidden within the noise. In particular we have applied the Singular Spectrum Analysis (SSA) that is designed to extract information from short and noisy time series and, thus, provide insight into the unknown, or only partially known, dynamics of the underlying system that generated the series (Ghil et al., 2000).

This methodology is analogous to applying an extended empirical orthogonal function analysis to successive lags of a univariate time-series and is equivalent to representing the behaviour of the system by a succession of overlapping "views" of the series through a sliding n-point window (Vautard et al., 2001). In so doing, the SSA allows the decomposition of the time series into a sequence of elementary patterns of behaviour that are classified as either trends or oscillatory patterns. From this decomposition into eigenvalues, it is possible to reconstruct each of the individual signals by adding the corresponding eigenvectors to the sample mean (Vautard et al., 2001).

3 Results

3.1 Annual time-series

The first set of comparisons is made considering the mean annual value of the different analysed variables in the two runs (RR and RN). Regarding hydrological conditions, both SST (sea surface temperature) and SSS (sea surface salinity) (Fig. 3A and B) are identical in both runs as it should be expected. These two variables depend on the external forcing to the model, i.e., atmospheric inputs and boundary conditions, which are equal in the two runs.

For biogeochemical variables (PPR and Chla) this is not true and, as shown in Fig. 3C and 3D, the RN mean values (red lines) are always lower than those from the RR. Even if the difference between the two runs looks quite constant in time in these two panels, the anomalies time series (RN – RR) shown in Fig. 3E indicate that both runs are more similar at the beginning of the simulation (until ~ 1970) with a mean difference of ~0.3% for PPR and ~4% for Chla. During the 1970s the difference sharply increases up to ~1.2% for PPR and ~8.7% for Chla. During the last two decades (~1990 to 2010) the differences remained high at ~1.1% for PPR and ~6.7% for Chla. These anomalies patterns are indicating that some factor strongly changed between the two model runs around the 1970s, which is when a substantial increase in biological productivity has been described for the basin (e.g., Macias et al., 2014b).

Figure 3. Mean annual values of model-simulated variables. A) Sea surface temperature (SST). B) Sea surface salinity (SSS). C) Integrated (120m) primary production rate (PPR). D) Surface (10m) chlorophyll-a concentration (Chla). E) Differences in PPR (blue) and Chla (green) between RR and RN.

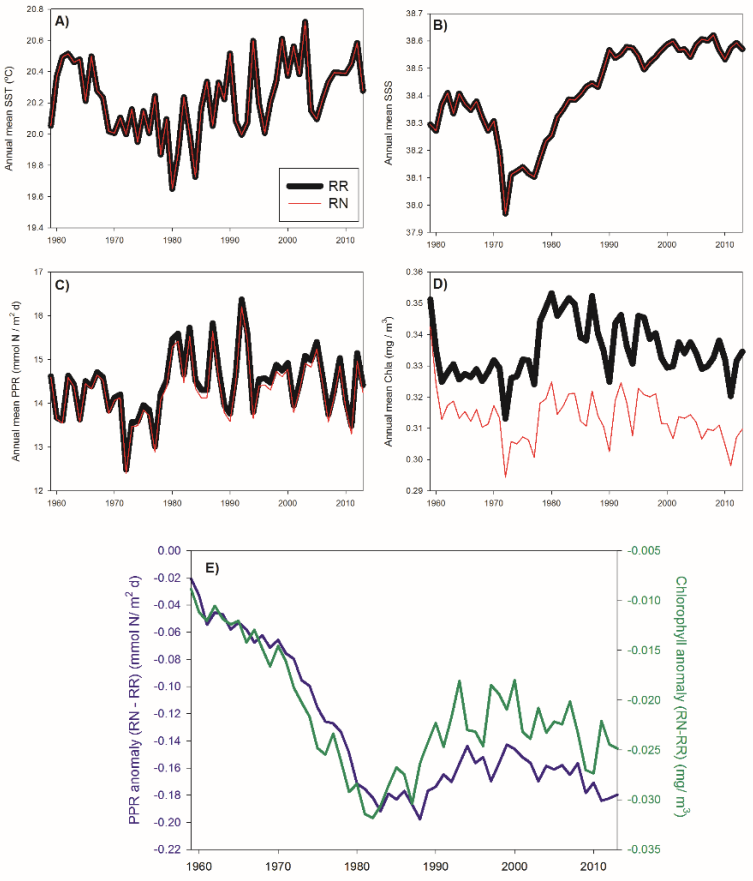

Another way of looking at differences of biogeochemical conditions in the two runs is analysing the time-series from Fig. 3C and 3D with a singular spectrum analysis (SSA, see details in methods). Results of this SSA decomposition are shown in Fig 4. For PPR in the RR, the main signal (accounting for ~14% of total variability) is very similar to the one identified in Macias et al., (2014b) and shows a clear transition from 'low productivity' towards 'high productivity' happening in the 1970s. The PPR series from the RN has a non-structured signal as the most energetic eigenvector (dotted line in Fig. 4A) containing around 13% of the total energy (i.e., very similar to the low-frequency signal identified for the RR). Only the third eigenvector shows a similar transition from low to high PPR (red line in Fig. 4A) but in this case it only represents ~11% of the total energy.

The differences in the SSA analysis of Chla are more evident (Fig. 4B). In the RR the main signal (with ~55% of the total energy) shows a clear increase during the 1970s with a marked peak ~1982 and a posterior decrease. For the RN, the main signal (~35% of the energy) shows a very different behaviour with constant oscillations showing different maxima along the series (red line in Fig. 4B). For the case of Chla in RN it was not possible to isolate a signal similar to the one found in the RR. It is also worth mentioning the much larger importance of these low frequency signal compared to those of the PPR where the amount of energy barely exceed 14%.

Figure 4. Singular spectrum analysis of the annual time series shown in Fig. 3. A) PPR and B) Chla

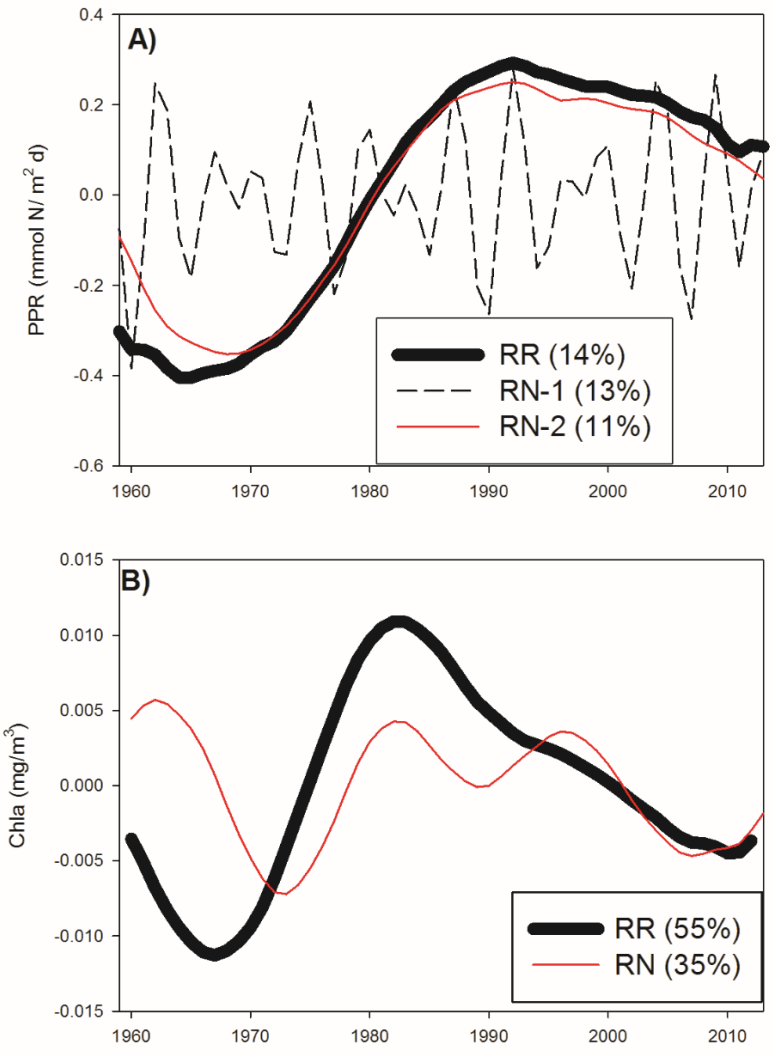

It is also possible to compare the anomalies maps for PPR and Chla in both runs (Fig. 5). Quite evidently, significant differences are only located in the vicinity of major rivers. Especially the Adriatic and Aegean basins are quite affected but also small regions around the Rhone, Ebro and Nile show significant impacts particularly for Chla concentration (Fig. 5B). The affected area is around 12% of the total Mediterranean if PPR is considered (Fig. 5A) and ~14% in terms of Chla (Fig. 5B) and the maximum anomalies could reach about 80 % for PPR and up to 95% for Chla in the Adriatic and Aegean seas. A detailed analysis of the differences in terms of primary production, phytoplankton biomass and bottom oxygen concentration in those three regions (Adriatic, Aegean and Gulf of Lion) for the two model runs could be found in Macias et al. (2018a). Also, these general patterns are quite similar to the ones found by Macias et al. (2016c) considering different rivers scenarios for 2030 but both the maximum differences and affected areas are much larger here, as could be expected for a total elimination of nutrients from the rivers' outflow.

Figure 5. Mean difference (RN – RR) in PPR (upper panel) and in Chla (lower panel) for the whole hindcast simulations. Non-significant differences are blanked

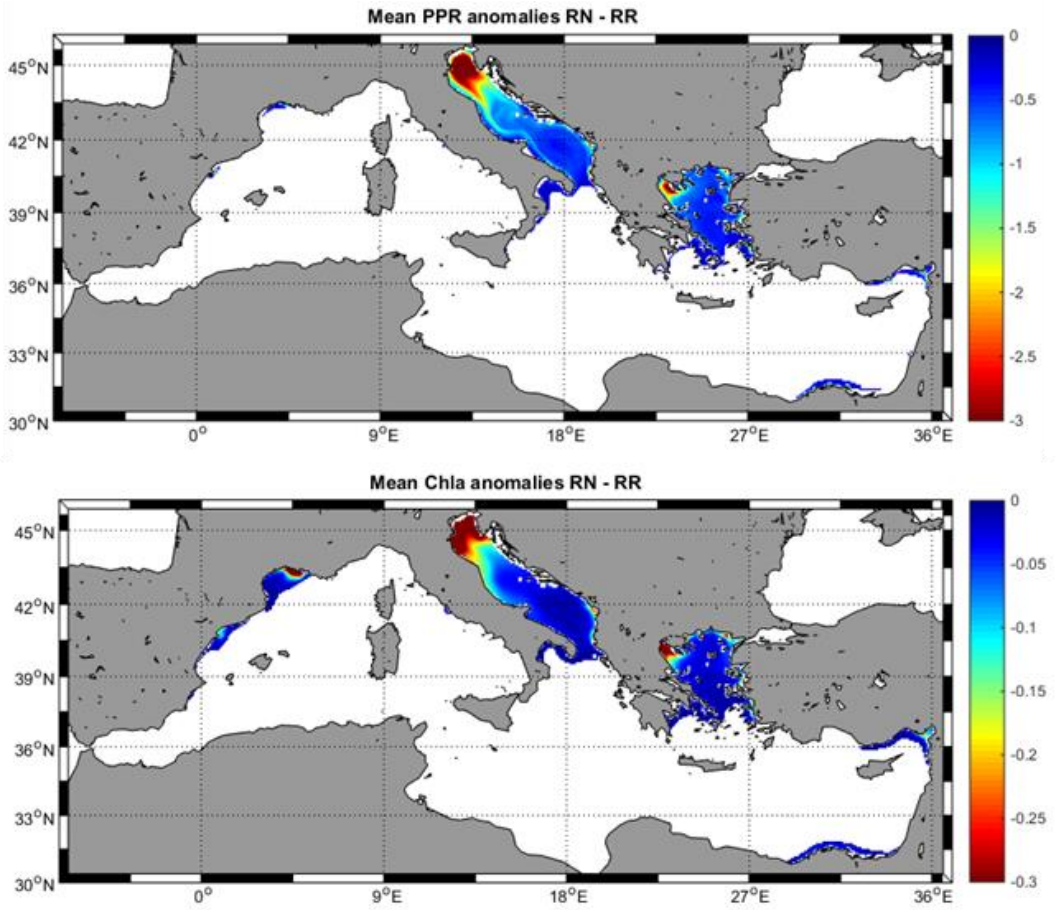

We can also compare the PPR and Chla anomalies maps (i.e., RN – RR) at the end of the simulation (2008 – 2013) and at the beginning (1960 – 1964) to understand where the differences shown by the anomalies time-series (Fig. 3E) are located. Such maps are shown in Fig. 6 and it could be seen that, evidently, the regions showing differences between the two time periods are, principally, the Adriatic and the Aegean seas. This provided further support to the hypothesis that the difference between the two periods

are due to the increase on production in the RR associated with the P and N increase in the rivers waters as shown in Macias et al. (2014b).

Figure 6. Difference in the anomalies (RN – RR) at the beginning of the simulations (1960 – 1964) and at the end (2008 – 2013) for PPR and Chla. Notice the PPR colorbar include positive values while Chla is always negative.

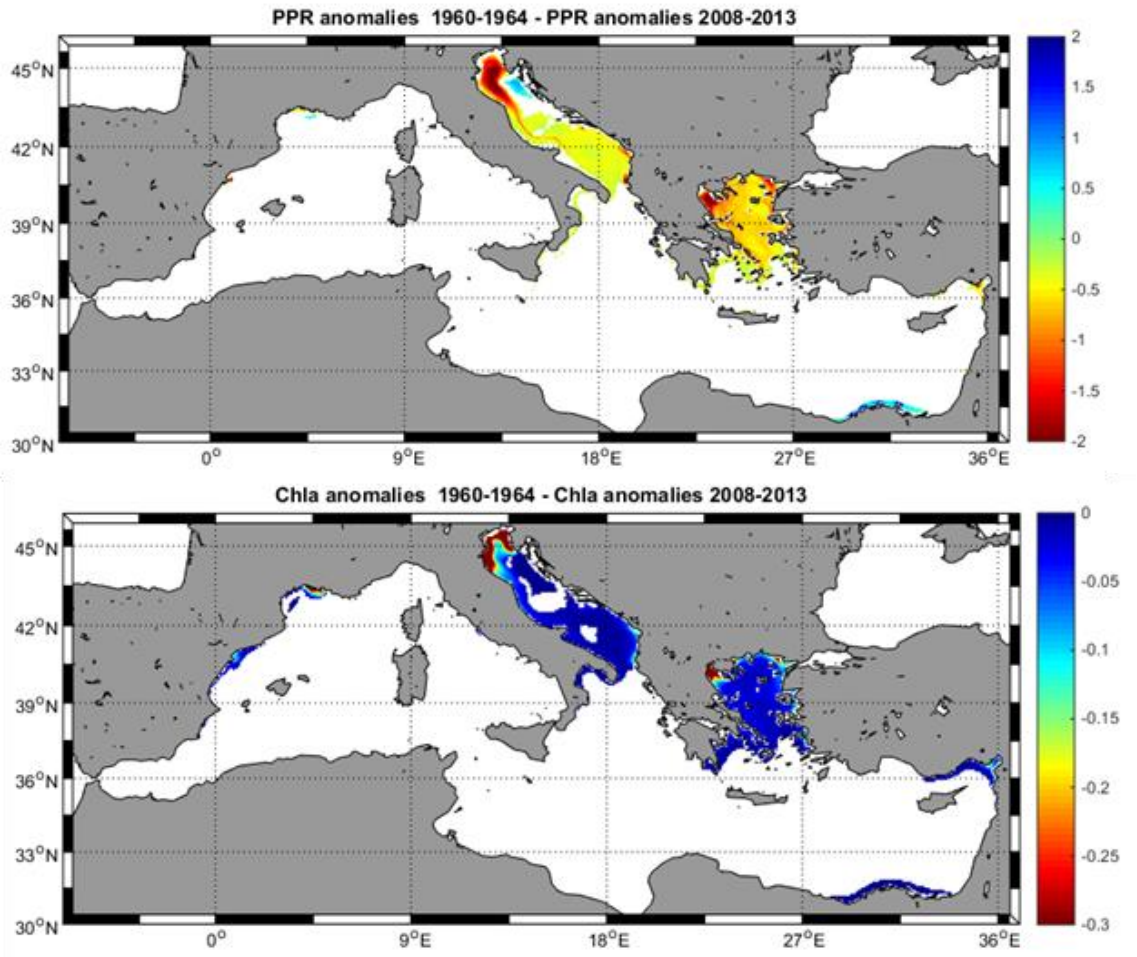

3.2 Seasonal differences

To further explore the differences between both runs, we have computed the seasonal cycles of PPR and Chla in the whole Mediterranean (Fig. 7). In both runs the seasonal pattern is, essentially, the same with a winter-spring production bloom, low biological activity during the summer-early fall and a later increase towards winter values. The relative difference between both runs (panel C of Fig. 7) seems to be maximum during the stratification period, and lower in the fall-winter months. During summer (when largest differences happen) vertical mixing and fertilization of the upper layer is reduced so the system is more dependent on allochthonous nutrient supply (i.e., rivers' fertilization).

It is also obvious that the most affected biological variable is the surface Chla, with mean differences ranging from 4 to 14% while PPR change between 0.8 and 1.2%. This is a quite obvious consequence of the different depth horizons considered for each variable, 10m for Chla and 120m for PPR. River-related differences usually happen around the rivers' mouths, so in shallow areas. Also integrated PPR is largely affected by open-sea processes in the Mediterranean as winter deep convection, wind-induced mixing and the

development of subsurface phytoplankton biomass maximum (especially during stratification period).

Figure 7. Seasonal cycle of PPR and Chla (panels A and B) for the two runs. Relative difference between the seasonal cycles (panel C)

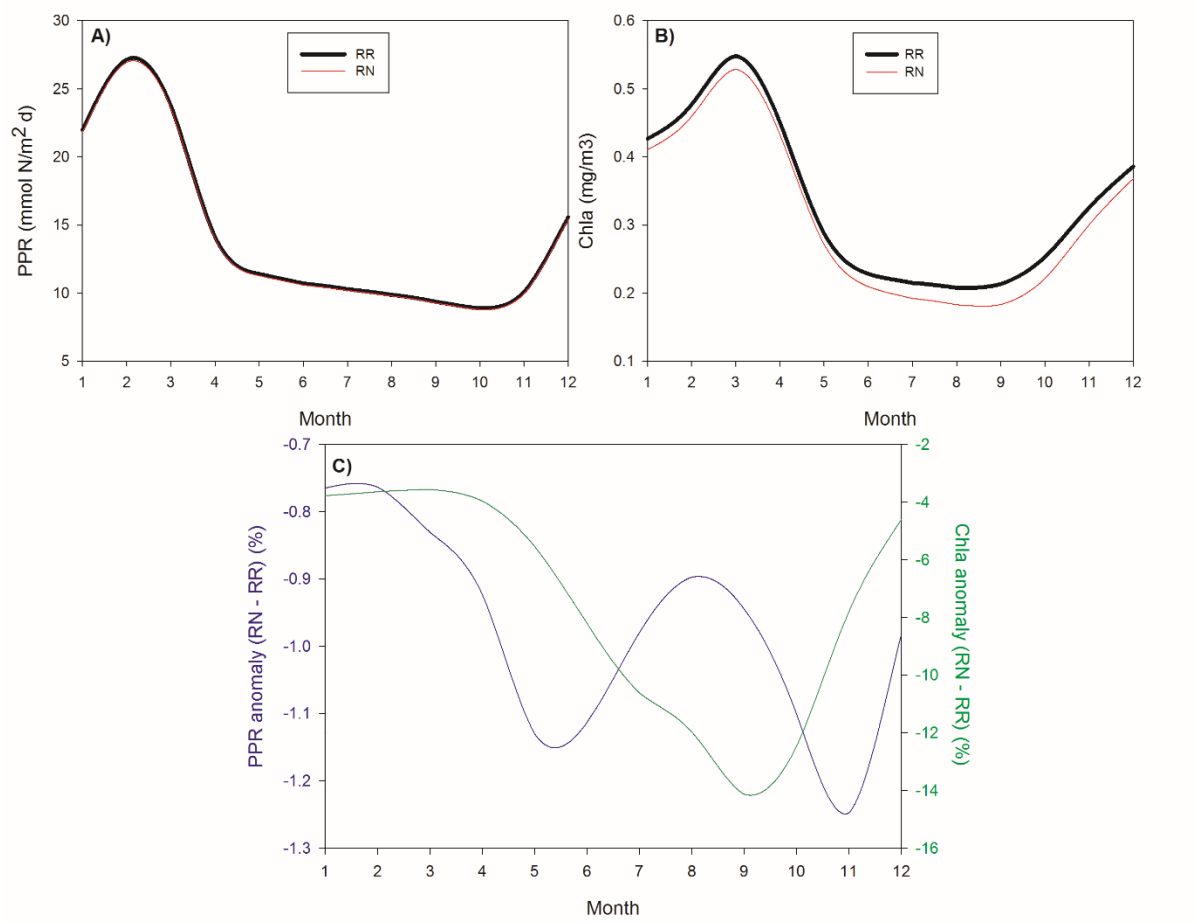

Comparing the anomaly maps for winter and summer (Fig. 8), no clear difference in the patterns could be seen. Basically the same regions described above for the climatological map (Fig. 4) are the most affected ones in the different seasons, only the mean value of the anomalies changes.

Figure 8. Mean winter (upper panel) and summer (lower panel) differences (RN – RR) for PPR and Chla

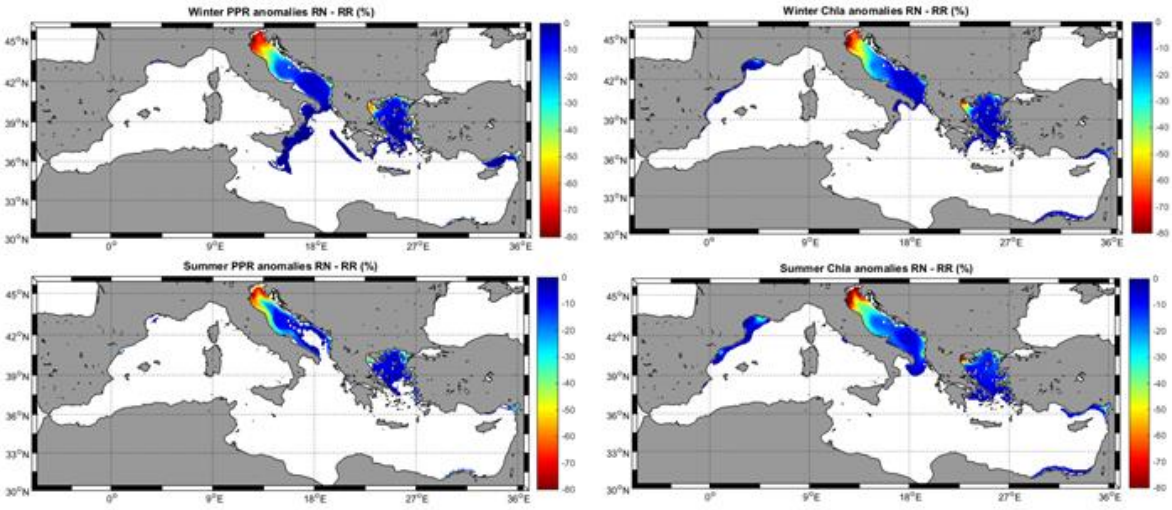

It is also possible to compute the anomaly time-series for each particular month (i.e., the monthly equivalent of Fig. 3A in relative values). For PPR (Fig. 9A) no clear seasonal differences could be observed with the individual monthly series (thin coloured lines) fluctuating around the mean (grey thick line). For Chla, however, the pattern is clearer (Fig. 9B) with maximum differences during summer- early fall (red thin lines). The mean summer difference (thick red line, Fig. 9B) started at around -7% and reached a maximum difference around 1981 at -17% fluctuating around -15% afterwards. For the winter months (thin blue lines) the mean difference (thick blue line) remains quite stable along the time series starting at ~2.3% and finishing at -4.4%. Spring months (magenta thin lines) lie somewhere in between the two previous ones. Again, it could be noticed that the relative importance of the river scenario is much larger (one order of magnitude) for surface Chla than for the integrated PPR.

Figure 9. Monthly anomalies time-series for PPR (A) and Chla (B). In panel B) thicker lines are the seasonal means including all months with the same color.

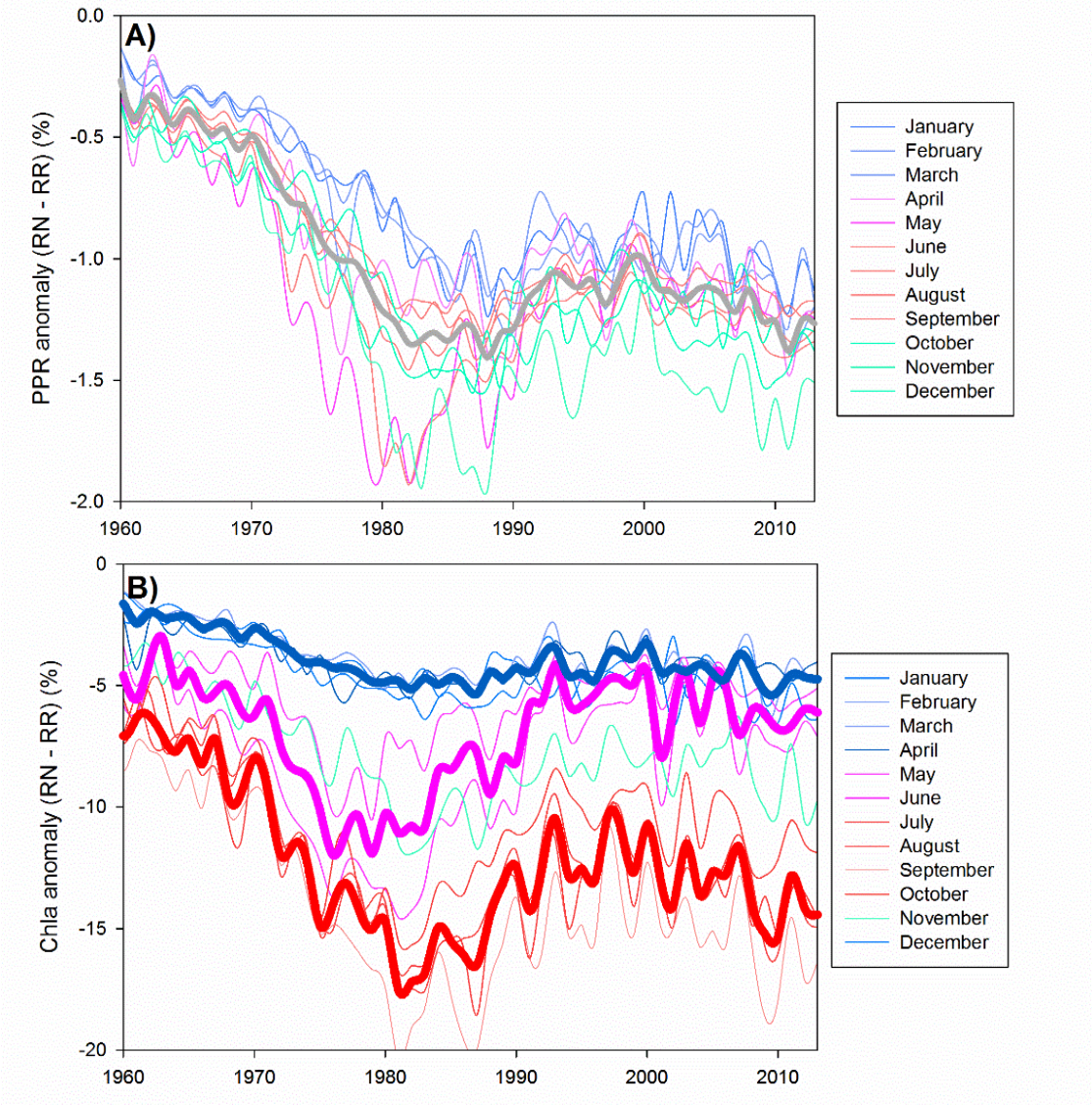

Given the larger impact of allochthonous nutrient supply on surface Chla, we repeated the spectral analysis on the monthly Chla time-series. Results for RR (Fig. 10A) show that only the central months of the year (May to October) present a low frequency signal similar to the one identified in the annual time-series (see Fig. 5B). All these individual signals (red thin lines in Fig. 10A) show a strong increase from the beginning to a maximum around 1980 – 1985 with a subsequent smaller decline towards the end of the time-series. The other months (blue thin lines in Fig. 10A) show no coherent low frequency signal or even a 4 years harmonic oscillation as the case of April (dotted blue line).

The same SSA performed for the RN shows how for most of the 'central' months (red lines in Fig. 10B) the low frequency signal described above is lost, only for May a slightly delayed similar signal could be found. In fact, the mean low frequency signal for those months (thick lines in Figs. 10A and B) change significantly as in RN there is a more continuous increase with several oscillations and no clear maximum in the 1980s.

Figure 10. Low frequency signals isolated by SSA from the monthly Chla time-series, from RR (A) and from RN (B). Months with similar low-frequency signal as the general one identified in Fig. X2 are drawn in red, the rest in blue. Thick red line is the mean signal of all 'red' months.

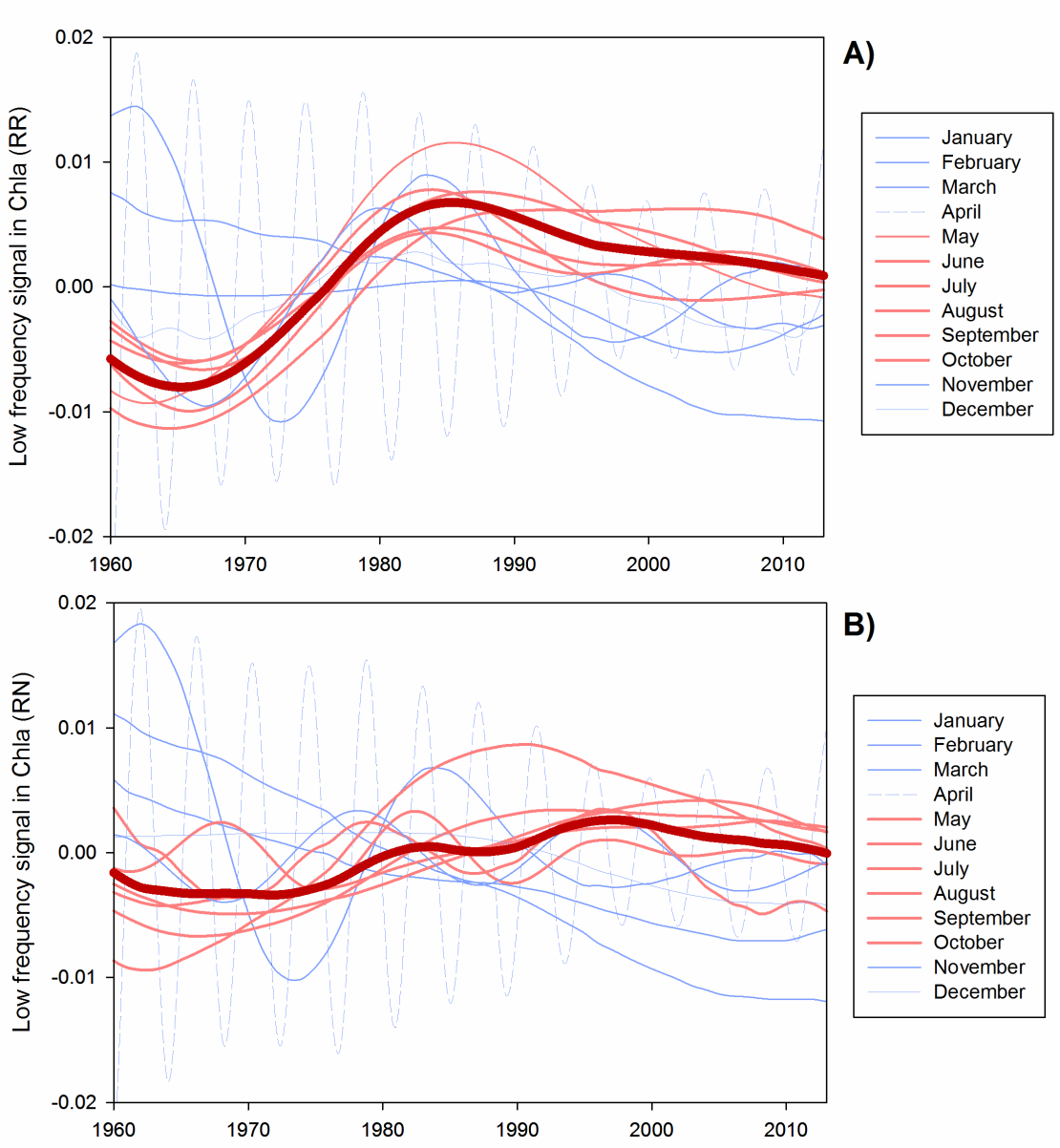

As a final comparison, the Chla maps for the 'central' months (red lines in Fig. 10) and for the winter season (blue lines in Fig. 10) are computed for the period 1981 – 1987 (when the red low frequency is more evident in RR) and compared in Fig. 11. The anomaly map (RN – RR) is quite similar for both 'seasons' (lower panels of Fig. 11) with the maximum differences in the Adriatic and Aegean Seas (max over 80%) and some noticeable (but smaller) change around the Rhone and Ebro rivers. However, there is a clear difference in the mean Chla pattern for both seasons as shown by the RR maps (upper panels of Fig. 11). During the stratification period (left column, Fig. 11) there are only substantial amounts of Chla around major rivers' mouths (excluding the Alboran Sea) while during winter, relatively high Chla concentrations could be found in the entire western Mediterranean corresponding with the blooming period (right panel, Fig. 11). Hence, when rivers nutrients are eliminated (i.e., the RN) the effect is relatively much larger in the stratification period than in the blooming one. This could explains why the low frequency signals for the 'central' months is more affected by the river scenario than the ones during the winter months (Fig. 10).

Figure 11. Mean Chla maps (upper and central rows) for the stratification months (left column) and for the winter season (right column). Lower row, mean difference for each 'season' computed as RN – RR. All maps correspond to the period 1981 – 1987.

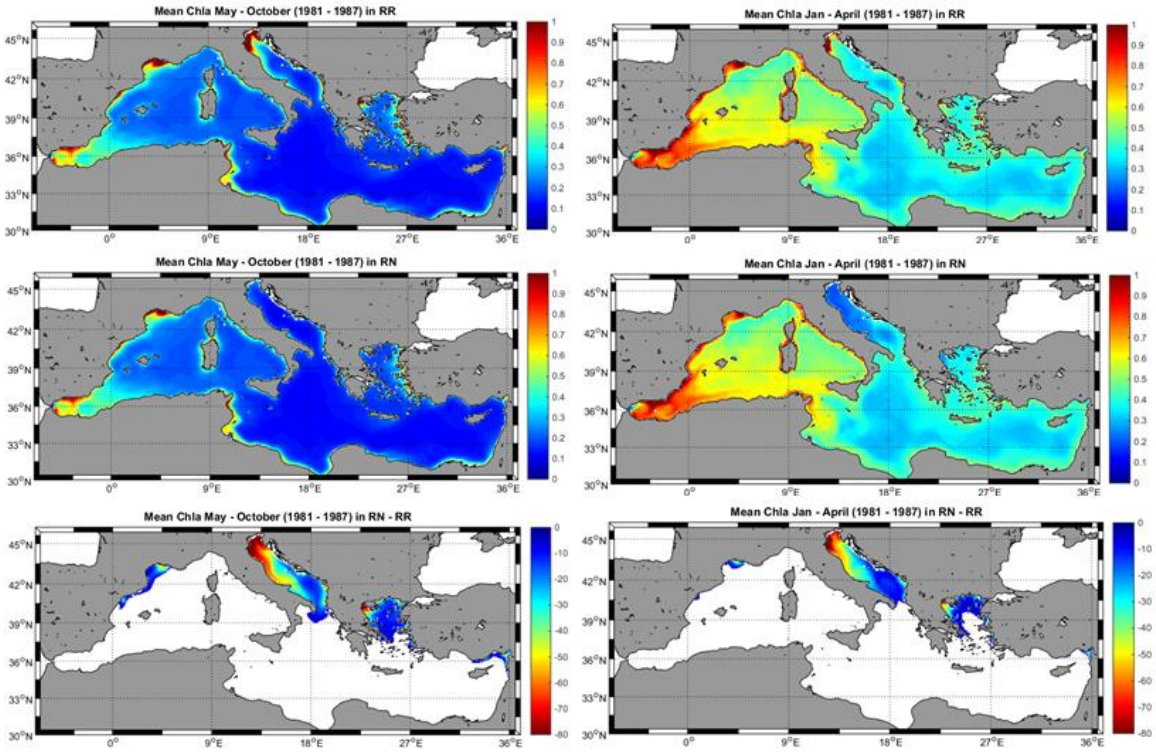

4 Discussion

Fromm the comparison of the two model runs, it is evident that the effect of river-borne fertilization is relatively larger for the surface Chla content (10m) than for the integrated (120m) PPR. For the later, the fertilization provoked by vertical mixing suppose a larger nutrient input maintaining the production levels in the basin.

The larger importance for surface properties of the rivers fertilization is also supported by the evident differences on mean anomalies between different seasons. Relative differences are larger for the summer (stratified months) than for the winter (mixing season) months. During the summer, the only biological production is found nearby the major rivers (Fig. 11, central panel) so removing nutrients from those have a larger impact on the overall productivity than in winter, when production is more widespread (Fig. 11, upper panel)

Interestingly, and related with this seasonal difference, we found that the low frequency signal in biological productivity for the last 50 years described in Macias et al. (2014b) is only evident in the stratified season (Fig. 10) being absent during the fall/winter months. This reinforces the idea of the larger importance of rivers' nutrient loads during the stratified season. It also supports the hypothesis about the rivers control of marine productivity in the Mediterranean as presented in this previous work.

Spatially and as expected, major differences between the RR and the RN runs are simulated in the vicinity of the major rivers (Fig. 6) with the Adriatic and Aegean Seas showing the largest anomalies. As shown by Macias et al. (2018a), in those regions not only pelagic production levels decrease when river fertilization is annulated but also bottom oxygen levels and hypoxic regions are altered. As also presented by Macias et al. (2018a), the main nutrient in the rivers responsible for the production (and associated hypoxia) is different in each region, being phosphate the most relevant one in the Adriatic and nitrate in the Aegean. Henceforth, measures to control eutrophication linked with freshwater inputs in each of these two basins should be, necessarily, different.

On the other hand, regions with enhanced marine productivity and located in the vicinity of the large rivers such as the Nile delta area and the Gulf of Lion are not that much affected by the removal of nutrients from the corresponding rivers (Figs. 6 & 11). The relative lack of response of coastal production levels in the Nile delta region could be related with a sub-optimal representation of the chemical conditions of this river in the RR as data availability is, certainly, low. The case of the Gulf of Lion has been extensively discussed by Macias et al. (2018b), as in here the major sources of nutrients for marine coastal production are the intense mesoscale processes typical of the region. Deep winter convection, strong slope currents and meandering induce large vertical mixing and fertilization of the water column. Rivers' effects here are limited to influence the stratification conditions in the coastal zone by the freshwater inputs (as discussed by Macias et al., 2018a).

The exhaustive comparison of the two contrasting simulations of rivers' chemical quality on the ecosystems conditions in the Mediterranean Sea here presented provides a baseline against which evaluate any alternative (intermediate) scenarios. Such scenarios could come, for example, from the programs of measures conducted by EU Member States in order to fulfil the Water Framework Directive (WFD) obligations on GES and Good Chemical Status of their freshwater bodies (Ferreira et al., 2011). The use of a holistic tool such as the MMF will help bringing the gap between different EU pieces of legislations (such as WFD and the Marine Strategy Framework Directive) providing an integrated, comprehensive evaluation of the involved ecosystems, their status and potential consequences on the services they provide.

References

Bruggeman, J., Bolding, K., 2014. A general framework for aquatic biogeochemical models. Environ. Modell. Software, 61: 249-265.

Burchard, H., Bolding, K., 2002. GETM, a general estuarine transport model, European Commission, Ispra, Italy.

Burek, P., van der Knijff, and A. de Roo. 2013. LISFLOOD - Distributed Water Balance and Flood Simulation Model - Revised User Manual. JRC technical report. Publications Office of the European Union. doi:10.2788/24719.

Ferreira, J. G., and others. 2011. Overview of eutrophication indicators to assess environmental status within the European Marine Strategy Framework Directive RID C-5701-2011. Estuar. Coast. Shelf Sci. 93: 117–131. doi:10.1016/ j.ecss.2011.03.014

Garcia-Gorriz, E., Macias, D., Stips, A., Miladinova-Marinova, S., 2016. JRC Marine Modelling Framework in support of the Marine Strategy Framework Directive: Inventory of models, basin configurations and datasets, European Commission, Luxemburg.

Ghil, M., Allen, M.R., Dettinger, M.D., Ide, K., Kondrashov, D., Mann, M.E., Robertson, A.W., Saunders, A., Tian, Y., Vadari, F., Yiou, P., 2002. Advanced spectral methods for climatic time series. Reviews of Geophysics, 40(1): 1-41.

Giorgi, F., 2006. Climate change hot-spots. Geophysical Research Letters, 33: L08707.

Ludwig, W., Dumont, E., Meybeck, M., Heussner, S., 2009. River discharges or water and nutrients to the Mediterranean and Black Sea: Major drivers for ecosystem changes during past and future decades? Prog. Oceanog., 80: 199-217.

Macías, D., García-Gorríz, E., Stips, A., 2013. Understanding the Causes of Recent Warming of Mediterranean Waters. How Much Could Be Attributed to Climate Change? Plos One, 8(11): e81591.

Macías, D., Stips, A., Garcia-Gorriz, E., 2014a. The relevance of deep chlorophyll maximum in the open Mediterranean Sea evaluated through 3D hydrodynamic-biogeochemical coupled simulations. Ecol. Model., 281: 26-37.

Macías, D., García-Gorríz, E., Piroddi, C., Stips, A., 2014b. Biogeochemical control of marine productivity in the Mediterranean Sea during the last 50 years. Global Biochemical Cycles, 28: 897-907.

Macías, D., Garcia-Gorriz, E., Stips, A., 2015. Productivity changes in the Mediterranean Sea for the twenty-first century in response to changes in the regional atmospheric forcing. Frontiers in Marine Science, 2(79).

Macías, D., Garcia-Gorriz, E., Stips, A. 2016a. The seasonal cycle of the Atlantic Jet dynamics in the Alboran Sea: direct atmospheric forcing versus Mediterranean thermohaline circulation. Ocean Dynamics, 66: 137-151.

Macías, D., Garcia-Gorriz, E., Stips, A., Dosio, A., Keuler, K., 2016b. Obtaining the correct sea surface temperature: bias correction of regional climate model data for the Mediterranean Sea. Climate Dynamics.

Macías, D., Stips, A.; Garcia-Gorriz, E. 2016c. Multi-year simulations of future socio-economic and climate scenarios in the Mediterranean Sea . EUR 28384 EN. Luxembourg (Luxembourg): Publications Office of the European Union. JRC103933

Macías, D., García-Gorríz, E., Stips, A., 2018a. Major fertilization sources and mechanisms for Mediterranean Sea coastal ecosystems. Limnol. Oceanogr., In press(63): 897-914.

Macías, D., García-Gorríz, E., Stips, A., 2018b. Deep winter convection and phytoplankton dynamics in the NW Mediterranean Sea under present climate and future (horizon 2030) scenarios. Sci. Reports, 8: 6626.

Macías, D., Stips, A., Garcia-Gorriz, E., Dosio, A., 2018c. Hydrological and biogeochemical response of the Mediterranean Sea to freshwater flow changes for the end of the 21st century. Plos One, 13(2): e0192174.

Markaki, Z., K. Oikonomou, M. Kocak, G. Kouvarakis, A. Chaniotaki, N. Kubilay, and N. Mihalopoulos. 2003. Atmospheric deposition of inorganic phosphorus in the Levantine Basin, eastern Mediterranean: Spatial and temporal variability and its role in seawater productivity. Limnol. Oceanogr. 48: 1557–1568. doi:10.4319/lo.2003.48.4.1557.

Neumann, T., 2000. Towards a 3d-ecosystem model of the Baltic Sea. Journal of Marine Systems, 25: 405-419.

Stips, A., Bolding, K. ,Pohlman, T., Burchard, H., 2004. Simulating the temporal and spatial dynamics of the North Sea using the new model GETM (general estuarine transport model). Ocean Dynamics, 54: 266-283.

Stips, A., Dowell, M., Somma, F., Coughla, C., Piroddi, C., Bouraoui, F., Macias, D., Garcia-Gorriz, E., Cardoso, A.C., Bidoglio, G., 2015. Towards an integrated water modelling toolbox, European Commission, Luxemburg.

Vautard, R., Yiou, P, Ghil, M., 1992. Singular Spectrum Analysis: A toolkit for short noisy chaotic signals. Phys. D., 58: 95-126.

List of abbreviations and definitions

AA: Administrative Arrangement
Chla: Chlorophyll -a
EEA: European Environmental Agency
ECMWF: European Centre for Medium-Range Weather Forecast
ERGOM: Ecological Regional Ocean Model
ETOPO1: Global Relief Model
DG JRC: Directorate General Joint Research Centre
FABM: Framework for Aquatic Biogeochemical Models
GES: Good Environmental Status
GETM: General Estuarine Transport Model
GRDC: Global River Data Centre
MEDAR/MEDATLAS: Mediterranean Data Archaeology and Rescue
MedERGOM: Mediterranean ERGOM
MMF: Marine Modelling Framework
MS: Member State
MSFD: Marine Strategy Framework Directive
PPR: Primary Production Rate
RESM: Regional Earth System Model
RN: Simulation without nutrients in rivers' water
RR: Simulation with realistic nutrients loads in rivers' water
SSA: Singular Spectral Analysis
WFD: Water Framework Directive

List of figures

GETTING IN TOUCH WITH THE EU

In person

All over the European Union there are hundreds of Europe Direct information centres. You can find the address of the centre nearest you at: https://europa.eu/european-union/contact_en

On the phone or by email

Europe Direct is a service that answers your questions about the European Union. You can contact this service:

- by freephone: 00 800 6 7 8 9 10 11 (certain operators may charge for these calls),

- at the following standard number: +32 22999696, or

- by electronic mail via: https://europa.eu/european-union/contact_en

FINDING INFORMATION ABOUT THE EU

Online

Information about the European Union in all the official languages of the EU is available on the Europa website at: https://europa.eu/european-union/index_en

EU publications
You can download or order free and priced EU publications from EU Bookshop at: https://publications.europa.eu/en/publications. Multiple copies of free publications may be obtained by contacting Europe Direct or your local information centre (see https://europa.eu/european-union/contact_en).

KJ-NA-29493-EN-N

The European Commission's science and knowledge service

Joint Research Centre

JRC Mission

As the science and knowledge service of the European Commission, the Joint Research Centre's mission is to support EU policies with independent evidence throughout the whole policy cycle.

EU Science Hub

ec.europa.eu/jrc

@EU_ScienceHub

EU Science Hub - Joint Research Centre

Joint Research Centre

EU Science Hub

Publications Office

doi:10.2760/045673

ISBN 978-92-79-98179-1